

The Dynamic Stabilization of the Rayleigh-Taylor Instability and the Corresponding Dynamic Equilibrium

G. H. WOLF*

Institut für Plasmaphysik, Garching bei München

Received July 2, 1969

Conditions are derived for dynamically stabilizing the Rayleigh-Taylor instability of a fluid interface and for attaining the corresponding dynamic equilibrium. These conditions could be proved in experiments using an aqueous solution of Potassium Jodide ($\rho_h=1.6 \text{ g/cm}^3$) as the heavy fluid and oil (viscosity SAE 140, $\rho_l=0.9 \text{ g/cm}^3$) as the light one. Parametric resonances were suppressed, but could be observed using oil of lower viscosity.

Introduction

The equilibrium of superposed fluids with a horizontal boundary is unstable if the density, ρ_h , of the upper fluid is greater than the density, ρ_l , of the lower one¹⁻⁴. Neglecting the effects of viscosity and surface tension and assuming the thickness, d , of the boundary layer to be small compared with the wavelengths, L , of the perturbations considered, the instability growth rate, Ω , was found to be¹⁻³

$$\Omega^2 = \frac{2\pi g}{L} \left(\frac{\rho_h - \rho_l}{\rho_h + \rho_l} \right). \quad (1)$$

Furthermore, if the boundary between the two fluids is not horizontal, no equilibrium exists at all.

* Institut für Plasmaphysik, Garching bei München, Germany. This work was performed as part of the joint research program between EURATOM and the Institut für Plasmaphysik GmbH, Garching, Germany.

1. Lord Rayleigh: Scientific Papers, ii, 200—207, Cambridge, 1900.
2. Taylor, G.: Proc. Roy. Soc. (London), Ser. A **201**, 192 (1950).
3. Lewis, D. J.: Proc. Roy. Soc. (London), Ser. A **202**, 81 (1950).
4. Chandrashekar, S.: Hydrodynamic and Hydromagnetic Stability. Oxford: Univ. Press 1968.

This paper describes a method of stabilizing the above mentioned instability and attaining stable equilibrium in the case of non-horizontal boundaries as well. An estimate of the stability conditions is derived, and experimental results showing the feasibility of this kind of stabilization are presented.

The Rayleigh-Taylor instability has also been considered for the case where the lower liquid is replaced by a magnetic field parallel to the boundary layer⁴ and the remaining fluid is of infinite electrical conductivity. This gives the connection to plasma physics, where macroscopic equilibrium and stability are usually analyzed by means of the so-called magneto-hydrodynamic (MHD) model. The experiments described in this paper thus also have some relevance to the attempts to stabilize dynamically⁵⁻¹⁴ MHD-unstable plasma configurations and to attain dynamic plasma equilibria¹⁵.

Stability

In order to stabilize the Rayleigh-Taylor instability, we enforce a harmonic oscillation of the frequency ω and amplitude a in the vertical direction upon the system containing the two fluids. This oscillation causes a periodic acceleration, \mathbf{b} , perpendicular to the horizontal boundary layer. The time dependence of the instantaneous acceleration acting on the fluids is then given by $\mathbf{g} + \mathbf{b}$, where

$$\mathbf{b} = b_{\max} \cos \omega t \quad (2)$$

and $b_{\max} = a\omega^2$.

5. Weibel, E. S.: Phys. Fluids **3**, 946 (1960).
6. Haas, F. A., and J. WESSON: Phys. Rev. Letters **19**, 833 (1967); — Culham Report CLM-P 188 (1968).
7. Troyon, F. S.: Phys. Fluids **10**, 2660 (1967); — Phys. Rev. Letters **19**, 1963 (1967).
8. Berge, G.: Conf. Proceedings, Novosibirsk, CN-24/J-11, I.A.E.A., Vienna (1969); — Conf. Proceedings, Utrecht, 77. Groningen: Wolters-Noordhoff Publ. 1969; — Culham Report CLM-R 97 (1969).
9. Demirkhanov, R. A.: Los Alamos Translation, LA-4056-TR (1969).
10. Ribe, F. L., and W. B. Riesenfeld: Phys. Fluids **11**, 2035 (1968).
11. Andelfinger, C., and G. Lehner: Garching Report IPP 1/77 (unpublished) (1968).
12. Gruber, O.: Verhandl. DPG (VI), 4, PP-23 (1969).
13. Bodin, H. A. B., E. P. Butt, J. McCartan, and G. H. Wolf: Conf. Proceedings Utrecht, 76. Groningen: Wolters-Noordhoff Publ. 1969.
14. Gribble, R. F., E. M. Little, W. E. Quinn, F. L. Ribe, G. A. Sawyer, K. S. Thomas, and D. M. Weldon: Conf. Proceedings Utrecht, 79. Groningen: Wolters-Noordhoff Publ. 1969.
15. Wolf, G. H., and G. Berge: Phys. Rev. Letters **22**, 1096 (1969).

The effective time-averaged potential, U_{eff} , of a single particle of mass m in a fast oscillating field with $\omega \gg \Omega$ is derived by Landau and Lifschitz¹⁶ to be:

$$U_{\text{eff}} = U_s + \frac{\overline{f^2}}{2m\omega^2}, \tag{3}$$

where U_s is the potential of the static case and f is the periodic force due to the oscillation. Applying Eq. (3) in a general way to our problem, where we consider a perturbation of the horizontal boundary with wave length L and amplitude ξ , the static potential becomes

$$U_s = U_0 - \frac{m}{2} \Omega^2 \xi^2, \tag{4}$$

where m is now the mass of the displaced fluids and U_0 is the arbitrary potential of the unperturbed boundary. The maximum value of the force f is given by $\partial U_s / \partial \xi$ when replacing g by b_{max} in the expression for Ω^2 , thus

$$f_{\text{max}} = \frac{b_{\text{max}}}{g} m \Omega^2 \xi. \tag{5}$$

Note that $\overline{f^2}$ is $f_{\text{max}}^2/2$. Combining Eqs. (3)–(5) yields

$$U_{\text{eff}} = U_0 - \frac{1}{2} m \Omega^2 \xi^2 + \frac{1}{4} \frac{m b_{\text{max}}^2}{g^2} \frac{\Omega^4}{\omega^2} \xi^2. \tag{6}$$

This leads to the stability condition

$$b_{\text{max}} \gtrsim \frac{2g^2}{a\Omega^2}. \tag{7}$$

Using the value of Ω from Eq. (1) yields

$$b_{\text{max}} \gtrsim \frac{Lg}{\pi a} \left(\frac{\rho_h + \rho_l}{\rho_h - \rho_l} \right). \tag{8}$$

Eq. (8) shows that the power necessary for stabilization increases, firstly with increasing wavelength of the perturbations, and secondly with decreasing difference in the density of the two fluids, the latter result being somewhat surprising.

16. Landau, L. D., u. E. M. Lifschitz: *Mechanik*, S. 108–110. Berlin: Akademie-Verlag 1962.

For practical applications, therefore, the smallest possible value of the instability growth rate, which can occur in a certain device, is of interest. This is found considering the lowest value of the oscillation frequency, Ω_0 , of standing surface wave modes in the stable case, where ρ_l is above ρ_h . Assuming the depths of the fluids to be large compared with the vessel diameter or greater lateral length, D , the value of Ω_0 for standing waves in a basin with bounded extent can be described by¹⁷

$$\Omega_0^2 = m_0 g \frac{\rho_h - \rho_l}{\rho_h + \rho_l}. \quad (9)$$

For a cylindrical vessel such that the fluid interface takes a circular cross section, the smallest value of m_0 is found at the first maximum of the Bessel-function $J_1(m_0 D/2)$. For a vessel of rectangular cross section, by contrast, the smallest value of m_0^2 becomes π^2/D^2 . This yields

$$\begin{aligned} m_0 &= 3.68/D && \text{circular cross section} \\ m_0 &= \pi/D && \text{rectangular cross section.} \end{aligned} \quad (10)$$

Consequently, the stabilization condition, for instance for the cylindrical vessel, becomes

$$b_{\max} \gtrsim 0.54 g \frac{D}{a} \left(\frac{\rho_h + \rho_l}{\rho_h - \rho_l} \right). \quad (11)$$

Parametric Resonances

Besides the Eqs. (7), (8), and (11), however, there is another restriction which has to be observed if no new instabilities are to be induced by the forced oscillations. The resulting criterion follows from the condition that the instantaneous growth rate should not exceed the value of ω , i. e. ω^2 has to be greater than the right hand side of Eq. (1) if g there is replaced by b_{\max} ($g \ll b_{\max}$). Hence for the smallest possible wavelength, L_{\min} , the growth rate of which can still be fairly described by Eq. (1), we obtain the condition

$$L_{\min} \gtrsim 2\pi a \left(\frac{\rho_h - \rho_l}{\rho_h + \rho_l} \right). \quad (12)$$

This demonstrates the necessity of physical mechanisms for suppressing fast growing short wavelength perturbations. Such mechanisms are

17. Wehausen, J. V., and E. V. Laitone: Encyclopedia of Physics, vol. IX, p. 623. Berlin-Göttingen-Heidelberg: Springer 1960.

provided by viscosity, surface tension or finite density gradient* in the boundary^{1,4}. The latter effect is of practical importance in plasma physics, where in the case of diffuse pressure profiles the short wavelengths can have about the same growth rate¹⁸ or can be damped¹⁹. However, even for wavelengths larger than L_{\min} some damping is required to prevent the development of parametric resonances, which would occur whenever $\Omega \approx n\omega/2$ (n positive integer). Those can be found using a more rigorous treatment which leads to Mathieu's stability chart²⁰. Note that the most dangerous case $n < 3$ is already covered by Eq. (12).

Dynamic Equilibrium

Furthermore, we are considering the situation where the forced oscillation is applied in the horizontal direction. The equilibrium position of the boundary is then no longer horizontal, but is at some angle, α , to the vertical. This case will be treated by analogy with the pendulum with horizontally oscillating support where¹⁶

$$\sin \alpha = \frac{2g^2}{a b_{\max} \Omega^2}. \quad (13)$$

Assuming this relation can be generalized to the case of fluids, and restricting ourselves to small values of α , we can use the Eqs. (9) and (10) to describe the value of Ω in a horizontally placed vessel with either circular or rectangular (vertical) cross section. This yields

$$\sin \alpha = 0.54 \frac{gD}{a b_{\max}} \left(\frac{\rho_h + \rho_l}{\rho_h - \rho_l} \right) \quad (14)$$

for the cylindrical vessel and

$$\sin \alpha = \frac{2}{\pi} \frac{gD}{a b_{\max}} \left(\frac{\rho_h + \rho_l}{\rho_h - \rho_l} \right) \quad (15)$$

for the rectangular one.

* R. S. Pease (private communication) has pointed out the problem that for small density gradients values of Ω can occur (even for short wavelength modes) which are smaller than Ω_0 as given by Eqs. (9) and (10).

18. Wobig, H.: Garching Report IPP 6/57 (unpublished) (1967).

19. Bodin, H. A. B., A. A. Newton, J. Wesson, and G. H. Wolf: Submitted for publication Phys. Fluids (1968).

20. Meixner, J., u. F. W. Schäfer: Die Grundlagen der mathematischen Wissenschaften, Bd. LXXI. Berlin-Göttingen-Heidelberg: Springer 1954.

When starting with a horizontal boundary surface, which is then exposed to the horizontally applied oscillation, a wave-like pattern of the surface will be excited. The eigenfrequency, Ω_s , of the standing surface waves is also described by Eq. (1) if we denote the quantity L to be the horizontal wavelength of the perturbations. Hence a rough estimate of α can be obtained in this case by combining the Eqs. (1) and (13) to give

$$\sin \alpha = \frac{g}{b_{\max}} \frac{L}{\pi a}. \quad (16)$$

Eq. (16), of course, is only valid for small amplitude waves. For large amplitude waves, by contrast, the Eq. (14) or (15) becomes relevant, although the value of Ω used there is no longer the correct one since the assumptions leading to Eq. (9) or (10) are violated in this case.

Experiments

Experimentally, a cylindrical glass vessel of inner diameter $D=2.8$ cm and axial length $A=6$ cm was mounted on a vibrator which applied oscillations to the vessel in the axial direction. The vessel was completely filled with equal quantities of an aqueous solution of Potassium-Iodide ($\rho_h=1.6$ g/cm³) and of a very viscous oil (SAE 140, $\rho_l=0.9$ g/cm³). The problem how to superpose the heavier fluid upon the lighter one was solved — after some other unsuccessful attempts — by starting off with the static stable arrangement, i. e. the oil on top. The vibrator was then adjusted to parameters expected to meet the conditions for dynamic stabilization [Eq. (11)] and for dynamic equilibrium [Eq. (14)]. It turned out that for the resulting value of $a^2 \omega^2$ the condition (12) was violated when oils of lower viscosity were used. With an oil of viscosity SAE 90, for instance, the plane boundary surface started to become covered with bubbles when for $\omega=3.5 \times 10^2$ sec⁻¹ the value of b_{\max} overcame 47 g. With oil of viscosity SAE 140, this effect was not observed up to $b_{\max}=60$ g, which was the greatest acceleration available from the vibrator. These oscillation parameters were maintained, and the whole device was placed in a horizontal position, where the boundary surface is determined by the dynamic equilibrium condition according to Eq. (14).

Photographs of the oscillating surfaces are shown in Fig. 1, a) with vertical cylinder axis and ρ_l above ρ_h , and b) with horizontally placed cylinder axis resulting in an inclined boundary surface. The exposure time was 10^{-1} sec, and a flash lamp synchronized with each oscillation was used to give a superposition of several single pictures.

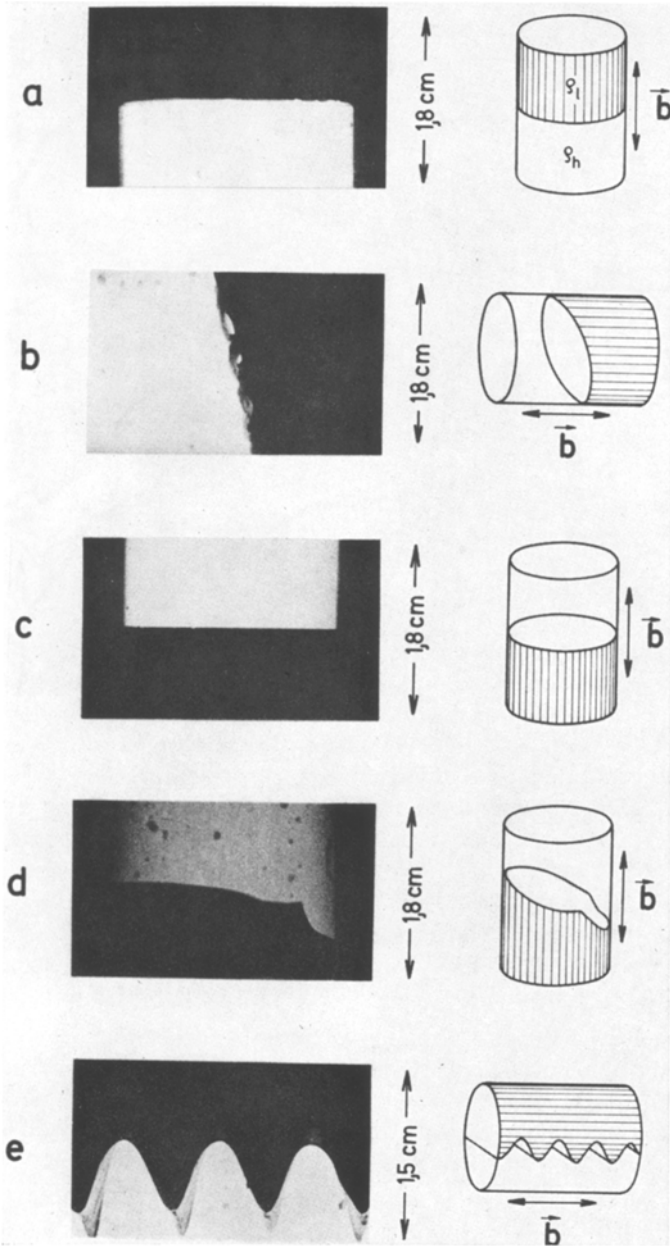


Fig. 1 a—e. Photographs showing the boundary surface of the fluids exposed to enforced oscillations in various directions a $\omega = 1.1 \pi \times 10^2 \text{ sec}^{-1}$, $b_{\text{max}} = 60 \text{ g}$, statically stable arrangement; b $\omega = 1.1 \pi \times 10^2 \text{ sec}^{-1}$, $b_{\text{max}} = 60 \text{ g}$, dynamic equilibrium separating the fluids horizontally; c $\omega = 2 \pi \times 10^2 \text{ sec}^{-1}$, $b_{\text{max}} = 60 \text{ g}$, statically unstable arrangement; d $\omega = 1.1 \pi \times 10^2 \text{ sec}^{-1}$, $b_{\text{max}} = 33 \text{ g}$, beginning of turbulent state; e $\omega = 2 \pi \times 10^2 \text{ sec}^{-1}$, $b_{\text{max}} = 40 \text{ g}$, wave-like pattern developing when surface originally horizontal

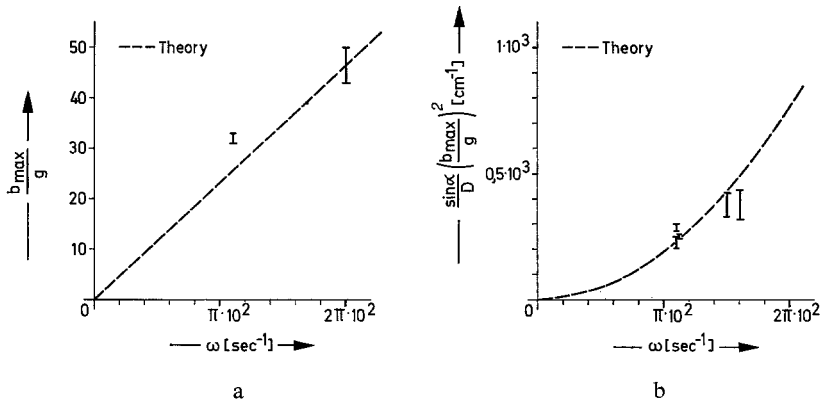


Fig. 2a and b. Experimental results compared with theoretical predictions a) for the condition of dynamic stabilization according to Eq. (11); b) for the relation of dynamic equilibrium according to Eq. (14)

Furthermore, from the horizontal position, Fig. 1b, the device was turned into the final state of ρ_h above ρ_l , i. e. where the Rayleigh-Taylor instability is dynamically stabilized. This case is shown in Fig. 1c for $\omega = 2\pi \times 10^2 \text{ sec}^{-1}$ and $b_{\max} = 60 \text{ g}$ since this higher frequency produces an even smoother and extremely plane surface compared with $\omega = 3.5 \times 10^2 \text{ sec}^{-1}$, where some (stable) surface waves could still be observed. The latter became more prominent in the horizontal case shown in Fig. 1b. There higher frequencies could not be used (keeping b_{\max} constant), since the value of α then increased until the surface began to split up into successive wedge-shaped parts and a sawtooth-like structure finally developed, each flank of which was again inclined towards the horizontal.

In the dynamically stabilized state (Fig. 1c) the value of b_{\max} could gradually be reduced until the stabilization condition was violated and the horizontal surface behaved like “slipping off”, leading to a turbulent interchange of the fluids. A photograph of this phase is shown in Fig. 1d, where, at $\omega = 3.45 \times 10^2 \text{ sec}^{-1}$, $b_{\max} = 33 \text{ g}$.

The last photograph in Fig. 1 shows an example of the wave-like pattern which is excited when the horizontal oscillation is applied to an originally horizontal surface; the particular parameters are $\omega = 2\pi \times 10^2 \text{ sec}^{-1}$ and $b_{\max} = 40 \text{ g}$. When the value of $a b_{\max}$ is increased the amplitudes and horizontal wavelengths of this pattern grow and change continuously into the above mentioned sawtooth structure. Preliminary quantitative results on dynamic stability and equilibrium are shown in

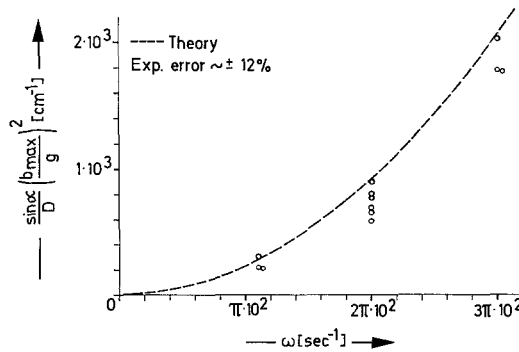


Fig. 3. Experimental results from the sawtooth-like structures excited by horizontal oscillations. The theoretical curve is derived from Eq. (15), where the quantity D is now the altitude of a sawtooth

Fig. 2, where on the left hand side (a) the value of b_{\max}/g is plotted versus ω ; the theoretically linear dependence is taken from Eq. (11). On the right hand side (b) the value of $\sin \alpha/D \cdot [b_{\max}/g]^2$ is plotted versus ω , and there the theoretical curve is derived from Eq. (14). The good agreement between the experimental results and the theoretical predictions shows firstly, that the simple model used for the calculations represents a fair description of the physical processes, and secondly, that viscosity and surface effects did not affect the gross dynamics of the fluids determined by the vessel diameter.

The wave-like or sawtooth-like patterns as shown in Fig. 1e have also been analyzed for various parameter values, and the results are plotted in Fig. 3. Although a quantitative description of this situation is based only on vague assumptions, the results were found to lie near the theoretical curve based on Eq. (15) and to deviate from the predictions based on Eq. (16) by less than a factor of two; better agreement was not expected in view of the more complex situation of that case.

The experiments described here are being extended in order to vary the essential parameters, to study the parametric resonances more extensively, and to investigate the stabilization of diffuse boundary layers.

Conclusion

It is concluded that the Rayleigh-Taylor instability can be dynamically stabilized, and that the corresponding dynamic equilibrium can be established, both for times which are long compared with the growth

times without oscillation. The quantitative results agreed with predictions based on simple physical models. Parametric resonances were only excited if the dominating viscosity was too low. These results encourage further attempts to stabilize dynamically MHD-unstable plasma configurations, which, like the Rayleigh-Taylor instability, have a whole spectrum of unstable modes, but where the growth rates of the short wavelength modes are also damped.

The author gratefully acknowledges helpful discussions with W. Engelhardt, Dr. G. Lehner, Prof. E. Schmid, and, in particular, Dr. D. Pfirsch. He is further indebted to G. Wendland for operating the vibrator, H. U. Scholz and E. Oberlander for assisting at the experiment and the Max-Planck-Institut für Extraterrestrische Physik for the use of the vibrator.

Dr. G. H. Wolf
Institut für Plasmaphysik
8046 Garching bei München